

SUPPLEMENTAL FIGURES AND LEGENDS

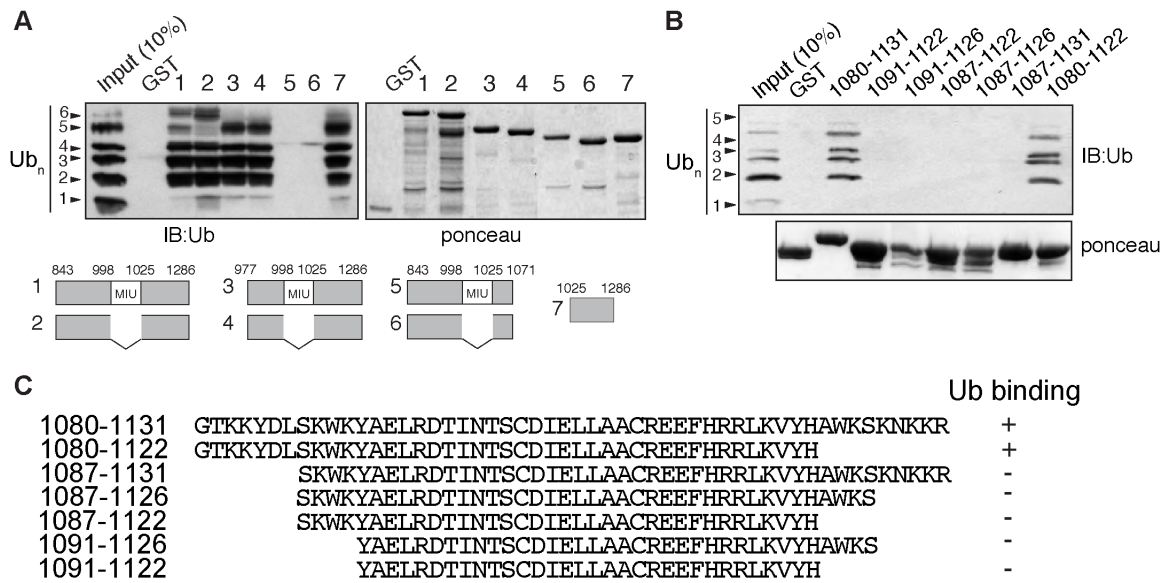
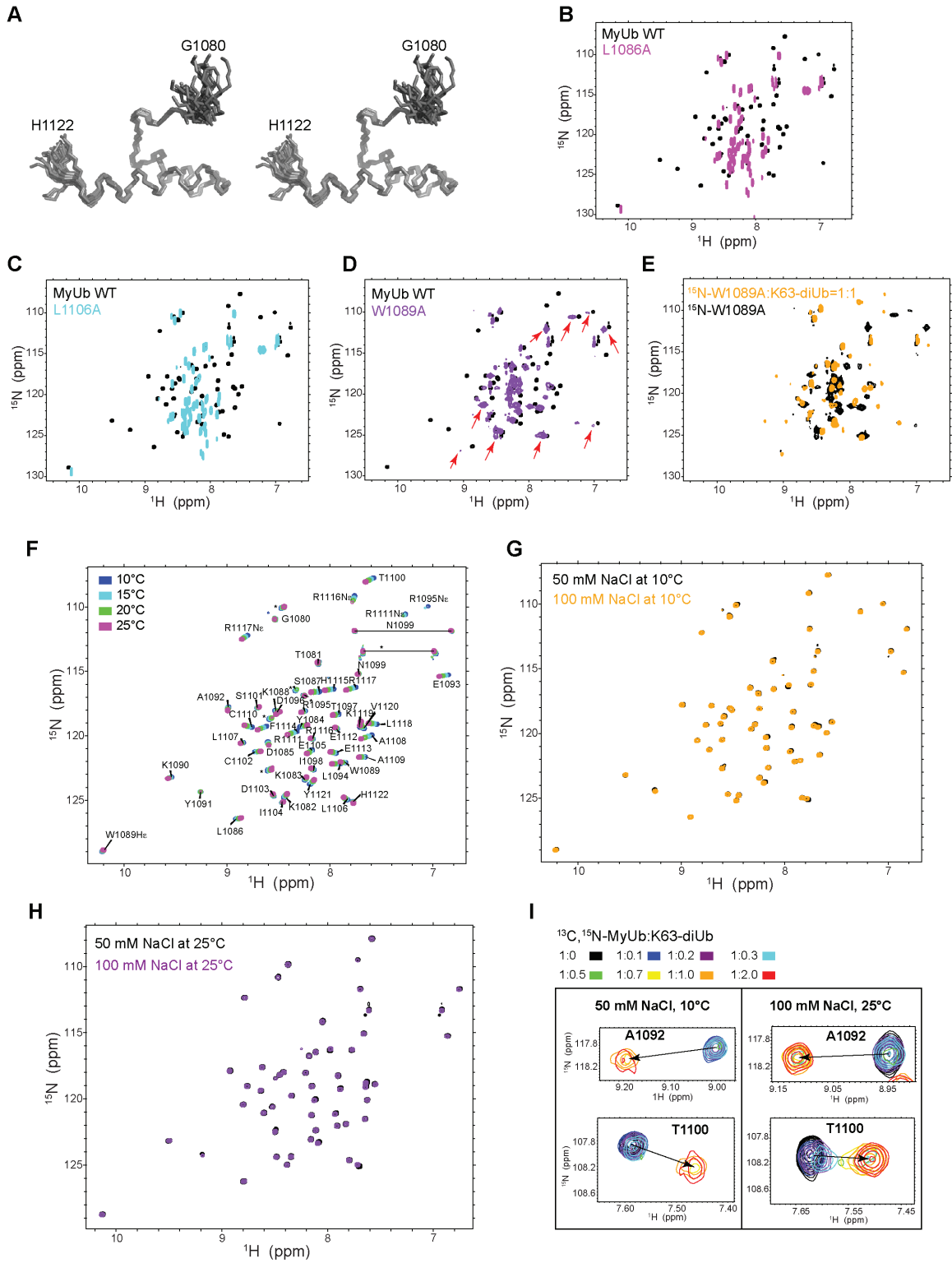


Figure S1. Identification and definition of MyUb domain boundaries, related to Figure 1.

(A) GST pull-down assays to evaluate ubiquitin binding for different myosin VI constructs, as indicated in cartoon representations at the bottom. GST fusion proteins were incubated at 4 °C for 2 hours with K63-linked polyubiquitin₁₋₇ and analyzed by immunoblotting (IB) with anti-ubiquitin antibody (left panel). GST is used as a negative control. Ponceau staining shows comparable loading of GST-tagged proteins (right panel).

(B) GST pull-down assay to evaluate ubiquitin binding of the indicated myosin VI deletion constructs. This experiment was performed as in (A).

(C) Amino acid sequences of the constructs used in (B) are displayed with ubiquitin binding capacity, as assessed in (B).



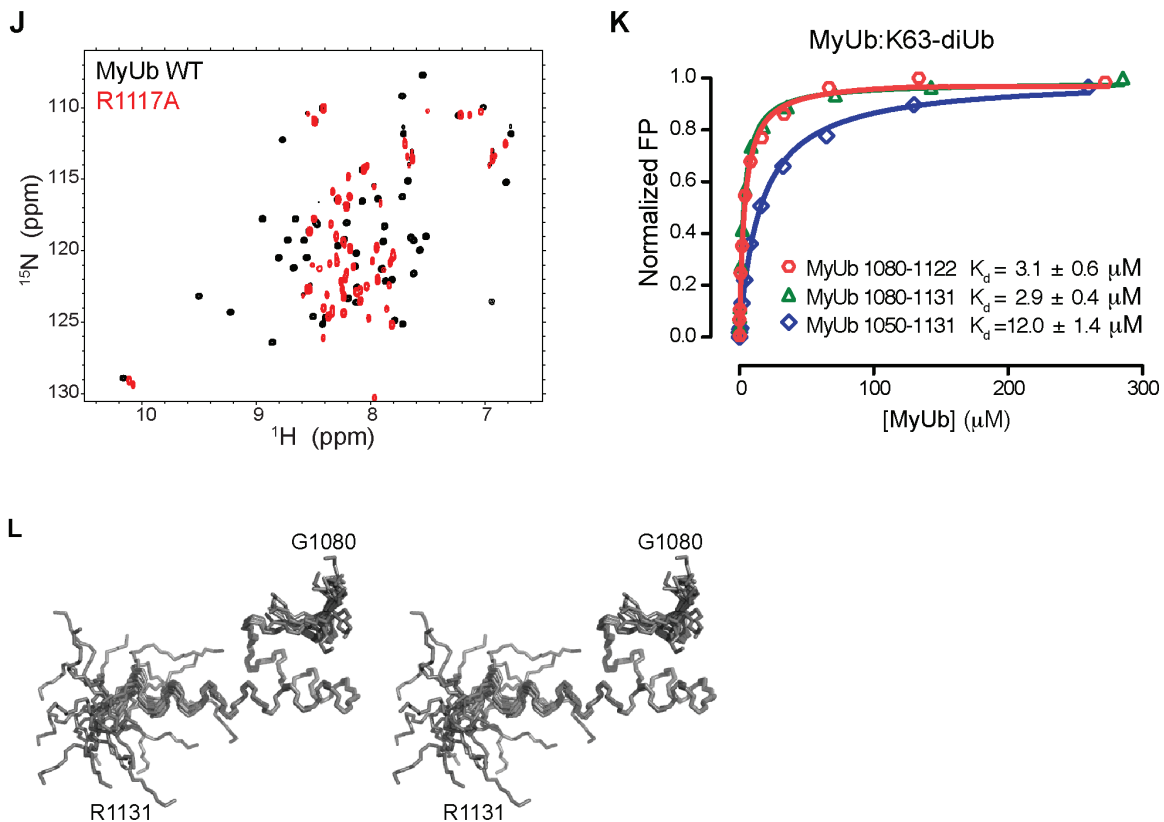


Figure S2. The MyUb fold and its critical amino acids, related to Figure 2.

(A, L) Stereoview of the twenty lowest energy structures from 100 extended starting ones for (A) MyUb (G1080-H1122) and (L) MyUb (G1080-R1131).

(B-D) ^1H - ^{15}N HSQC spectra of ^{15}N -labeled MyUb (G1080-H1122, black) and with (B) L1086, (C) L1106, or (D) W1089 substituted with alanine. The dispersed signals marked by red arrows indicate that the W1089A substitution does not completely disrupt the protein fold. The spectra were acquired at 600 or 850 MHz with samples of 0.1-0.2 mM in NMR buffer.

(E) ^1H - ^{15}N HSQC spectra of ^{15}N labeled MyUb W1089A (G1080-H1122, black) and after adding equimolar unlabeled K63-linked diubiquitin (orange). The spectra were acquired at 600 MHz with a sample of 0.1 mM in NMR buffer.

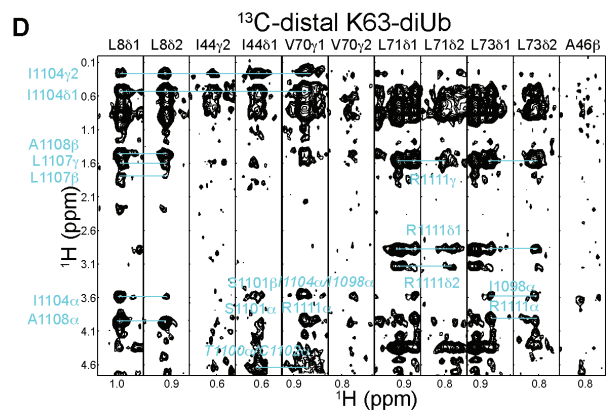
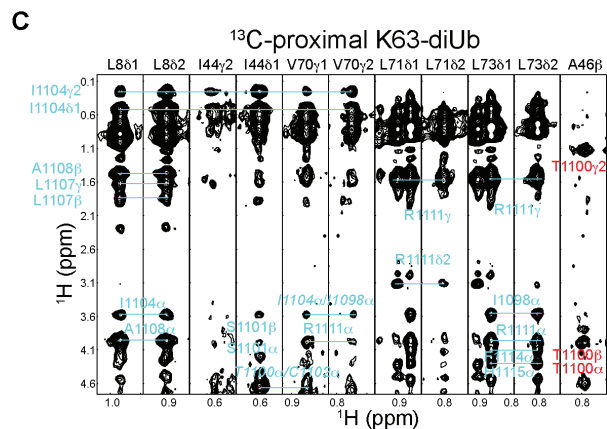
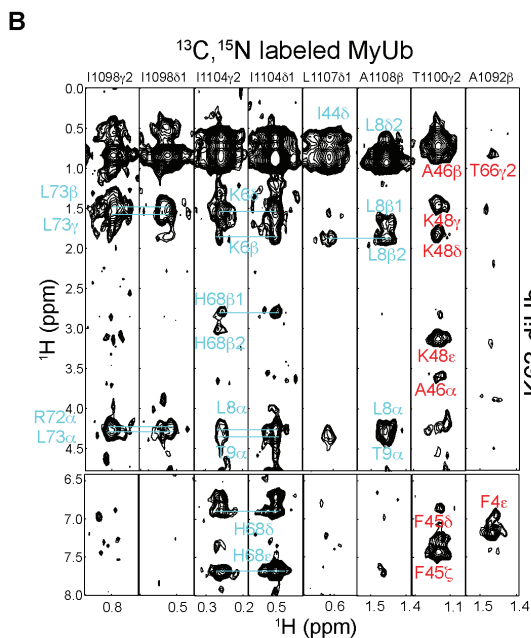
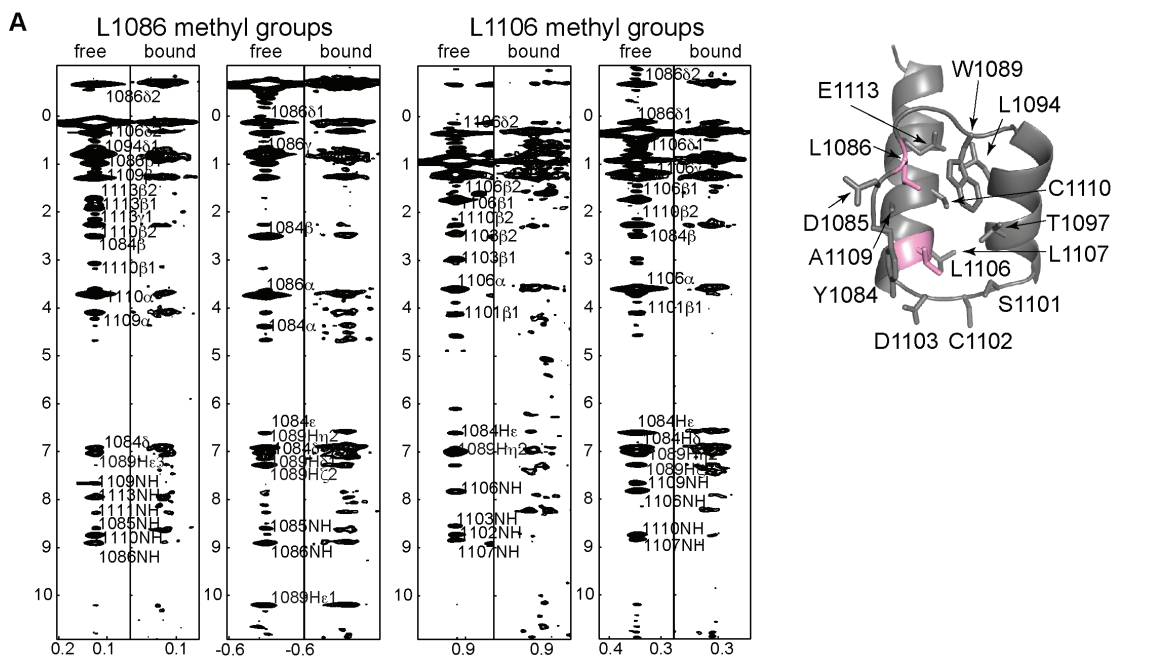
(F) ^1H - ^{15}N HSQC spectra of ^{15}N labeled MyUb acquired on 600 MHz with 0.22 mM protein sample in NMR buffer at different temperatures, as indicated.

(G-H) Superposition of ^1H - ^{15}N HSQC spectra of ^{13}C , ^{15}N labeled MyUb at NMR buffer with 50 or 100 mM NaCl at (G) 10°C or (H) 25°C. The spectra were acquired at 600 MHz with a sample concentration of 0.1 mM.

(I) Selected regions illustrating A1092 and T1100 signals from ^1H - ^{15}N HSQC spectra acquired on ^{15}N -labeled MyUb in phosphate buffer (pH 6.5) with 50 mM NaCl at 10°C (left) or 100 mM NaCl at 25°C (right) and with K63-linked diubiquitin at the indicated molar ratio. Arrows indicate new peak positions caused by addition of K63-linked diubiquitin. The spectra were acquired at 600 MHz with a sample of 0.1 mM MyUb concentration.

(J) ^1H - ^{15}N HSQC spectra of ^{15}N -labeled MyUb (G1080-H1122, black) and with R1117 substituted with alanine (red). The spectra were acquired at 700 MHz on 0.1 mM MyUb in NMR buffer.

(K) Fluorescence polarization (FP) experiments with resulting binding affinities listed for MyUb G1080-H1122, MyUb G1080-R1131, or MyUb R1050-R1131 binding to K63-linked diubiquitin, along with K_d values.



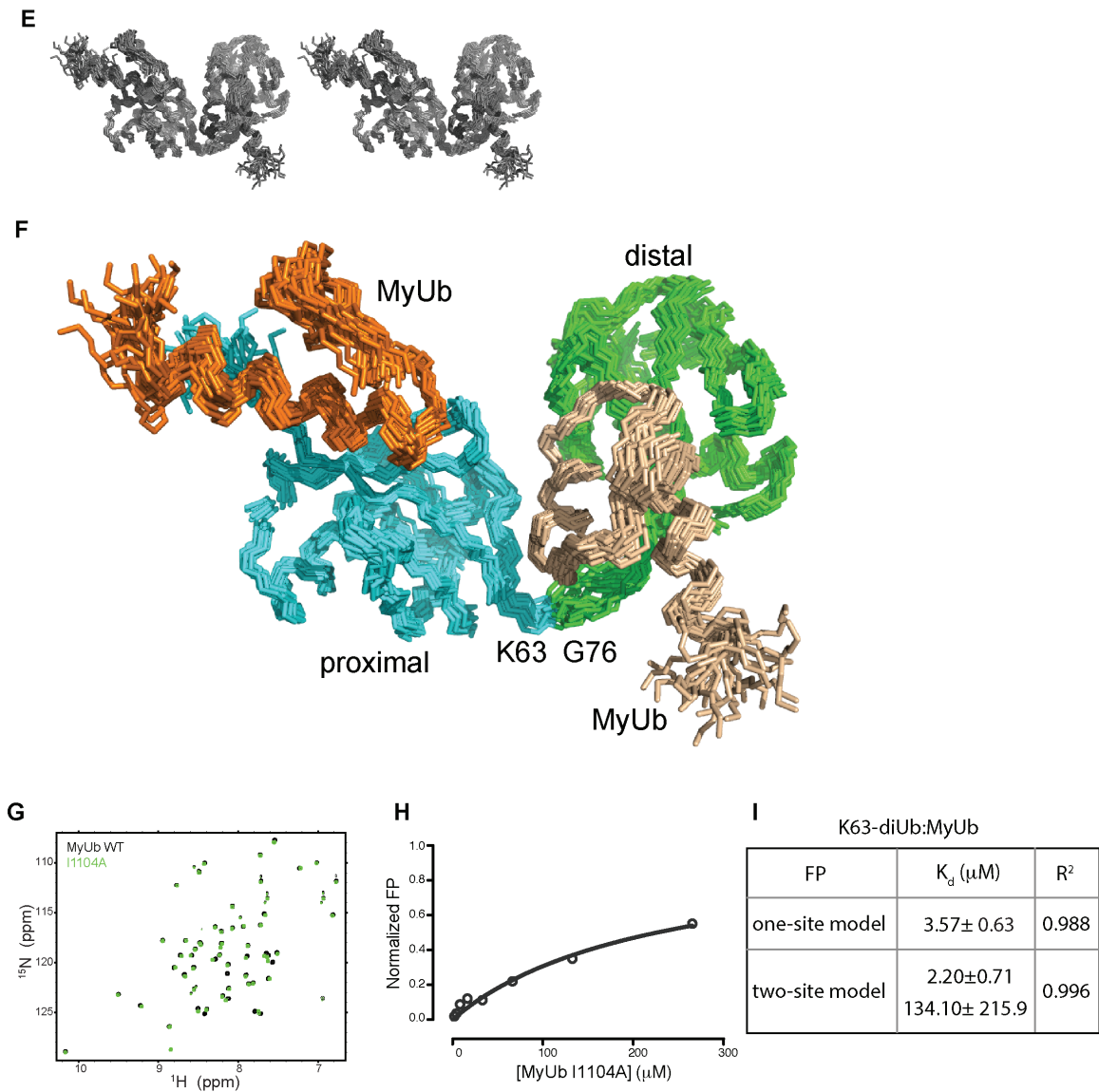


Figure S3. MyUb binds to K63-linked diubiquitin with distinct interactions to distal and proximal ubiquitin, related to Figure 3.

(A) Regions from a 3D ^{13}C -dispersed NOESY spectrum displaying MyUb methyl groups from the hydrophobic core (L1086 and L1106) in the absence (free) and presence (bound) of K63-linked diubiquitin; these amino acids and those that they show NOE interactions to are displayed to the right on a ribbon representation of MyUb (G1080-H1122). The spectra were acquired at 850 MHz with a sample of 0.3 mM concentration dissolved in NMR buffer.

(B) Selected regions from a 3D ^{13}C half-filtered NOESY spectrum acquired on ~ 0.6 mM ^{15}N , ^{13}C MyUb (G1080-H1122) in NMR buffer at 900 MHz with equimolar unlabeled

K63-linked diubiquitin highlighting intermolecular NOE interactions. NOEs assigned uniquely to proximal ubiquitin are labeled in red.

(C-D) Selected regions of 3D ^{13}C half-filtered NOESY spectra acquired with unlabeled equimolar MyUb (G1080-H1122) and K63-linked diubiquitin with ^{13}C -labeled (C) proximal or (D) distal ubiquitin. Assignments are indicated with those unique to proximal ubiquitin labeled in red. The protein samples were in the same condition as in (A) and the data were collected at 900 MHz. NOE interactions belonging to more than one amino acid pair are labeled in italics.

(E) Stereoview of the twenty lowest energy structures from 100 extended starting structures for MyUb (G1080-H1122):K63-linked diubiquitin.

(F) Twenty calculated structures of MyUb (G1080-H1122):K63-linked diubiquitin with two MyUb molecules bound to one K63-linked diubiquitin. One MyUb (beige) nestles between proximal (blue) and distal (green) ubiquitin as the other MyUb (orange) binds to the hydrophobic patch of proximal ubiquitin.

(G) ^1H - ^{15}N HSQC spectra of ^{15}N -labeled MyUb (G1080-H1122, black) and with I1104 substituted with alanine (green). The spectra were acquired at 700 MHz on 0.1 mM protein samples in NMR buffer.

(H) FP assays to analyze MyUb I1104A binding affinities for K63-linked diubiquitin. Based on the fact that the curve does not reach saturation, the dissociation constant can be inferred to be $>400 \mu\text{M}$.

(I) Table of K_d and R^2 values of one representative FP experiment of MyUb binding to K63-linked diubiquitin. Values were obtained by fitting the data with a two-site (as shown in Figure 1E) or one-site interaction model. The better fit with the two-site model indicates the presence of a second binding site at low affinity for MyUb on K63-linked diubiquitin (shown in orange in panel F).

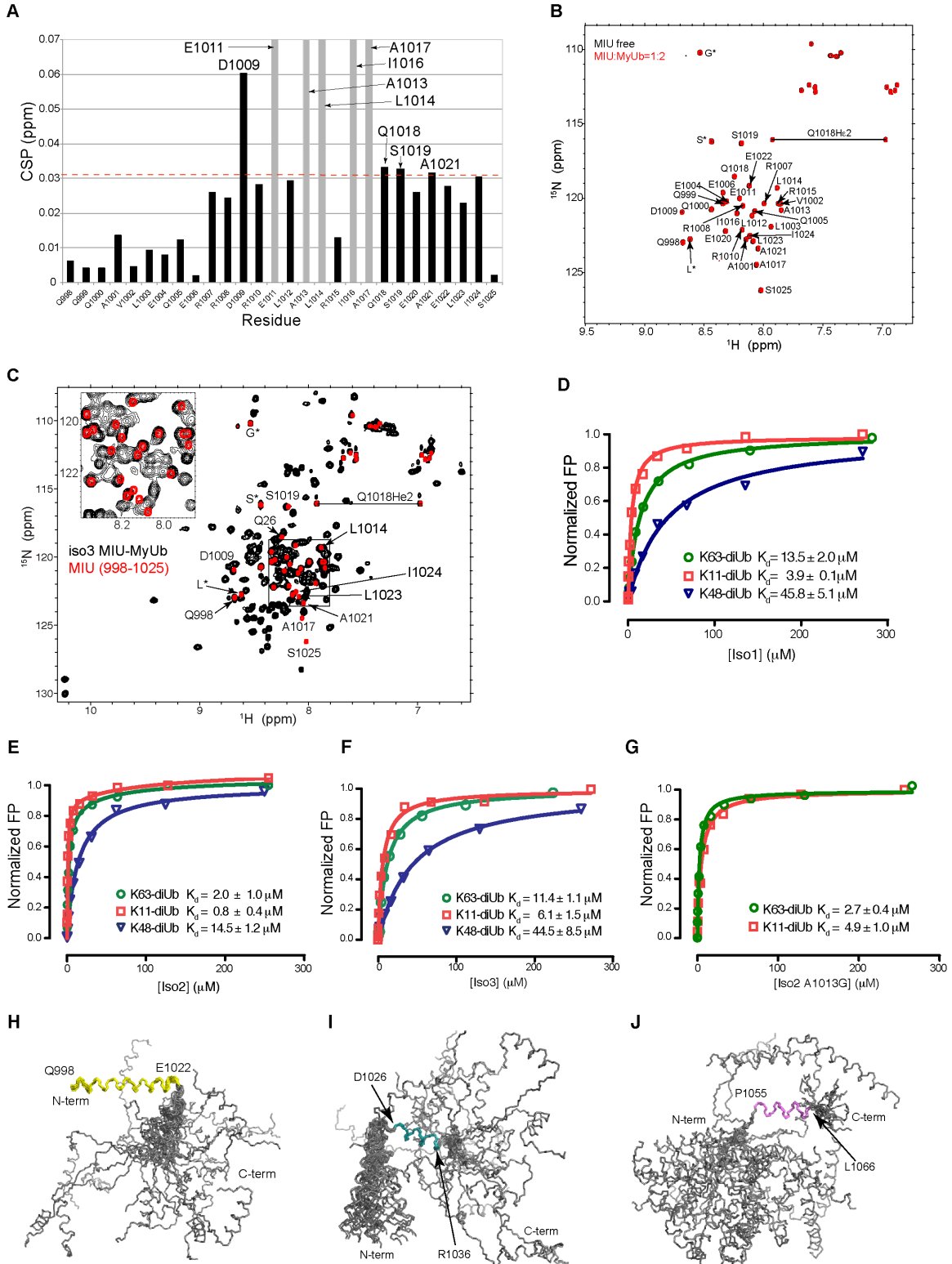


Figure S4. Features of the MIU region, related to Figure 6.

(A) CSP data for Figure 6B, in which 0.1 mM ^{15}N labeled MIU interacts with ubiquitin at 1:2 molar ratio. Amino acids that disappear during the titration are illustrated with gray bars. One standard deviation above average is indicated by a red dashed line.

(B) 2D ^1H - ^{15}N HSQC spectra of ^{15}N -labeled MIU (Q998-S1025, black) and with unlabeled MyUb at 2-fold molar excess (red). Data were collected on 850 MHz in 0.1mM protein sample in NMR buffer. Asterisks indicate signals derived from amino acids remaining after cleavage of the purification tag (GPLGS).

(C) Superimposed 2D ^1H - ^{15}N HSQC spectra of ^{15}N labeled iso3 (Q998-R1131, black) with ^{15}N labeled MIU (Q998-S1025, red). An expansion of the crowded region is included and asterisks indicate signals from amino acids left by the purification tag (GPLGS).

(D-G) FP measurements and listed binding affinities for MIU-MyUb constructs from (D) iso1, (E) iso2, (F) iso3, or (G) iso2 A1013G binding to K11-, K48-, or K63-linked diubiquitin, along with K_d values. Curves are representative of at least three independent experiments.

(H-J) Twenty lowest energy structures from 100 extended starting structures for iso3 Q998-A1071 superimposing (H) the MIU (Q998-E1022, yellow), (I) linker- α 1 (D1026-R1036, blue), or (J) linker- α 2 (P1055-L1066, purple). N-term, N-terminus; C-term, C-terminus.

Table S1. Structural statistics for MyUb (G1080-H1122), MyUb (G1080-R1131), MyUb (G1080-H1122):K63-linked diubiquitin, and iso3 Q998-A1071, related to Figure 2, 3, and 6.

	MyUb ^a (1080-1122)	MyUb ^b (1080-1131)	MyUb ^a :K63-diUb ^c (1:1)		Iso3 ^d 998-1071
			Proximal	Distal	
NOE restraints					
Total	880	815	2716	2727	1220
Intra-residue	281	251	418	421	374
Sequential ($ i - j = 1$)	250	251	345	345	432
Medium-range ($1 < i - j < 5$)	229	205	315	315	408
Long-range ($ i - j \geq 5$)	120	108	1638	1646	6
Intermolecular NOE	-		59	47	
Hydrogen bonds	20	25	-	-	36
ϕ/ψ dihedral angle	27/27	32/32	42/42	42/42	55/58
CYANA target function (\AA^2)	0.006	0.49	2.02		0.12
Violations					
Number of NOE $> 0.20 \text{ \AA}$	0	0	1		0
Max. NOE violation value (\AA)	0.18	0.15	0.24		0.15
Number of dihedral angle $> 2.5^\circ$	0	0	0		0
Max. dihedral angle violation value ($^\circ$)	0.79	2.13	1.51		0.40
Average total energy (kcal mol^{-1})	52.607	73.68	303.521		73.97
Ramachandran plot statistics					
Most favored regions (%)	86.4	89.1	80.0		99.2
Additional allowed regions (%)	13.6	10.9	19.1		0.8
Generously allowed regions (%)	0.0	0.0	0.9		0.0
Disallowed regions (%)	0.0	0.0	0.0		0.0
RMSD (\AA)					
Backbone	0.20	0.15	0.76		0.26
Heavy atoms	0.79	0.92	1.00		1.00

The regions for Ramachandran plot statistics and RMSD calculations include (a) D1085-K1119, (b) D1085-K1119, (c) M1-L73, and (d) Q998-A1021.

SUPPLEMENTAL EXPERIMENTAL PROCEDURES

Reagents, Antibodies, Constructs and Cell Lines. Reagents include unlabeled ubiquitin (SIGMA), K48- and K63-linked ubiquitin chains (1-7 moieties, Enzo Life Sciences), diubiquitin (M1, K6, K11, K27, K29, K33, K48, K63, Boston Biochem, Inc.), Antibodies include: anti-ubiquitin antibodies (P4D1, Santa Cruz Biotechnology and ZTA10, generated in-house), anti-HA (clone 16B12, Convance), anti- GFP (G1544, Sigma), GFP-Trap (Chromotek).

GFP-optineurin, FLAG-T6BP, His-GIPC, and FLAG-NDP52 were generously provided by Dr. Alain Israel, Dr. Folma Buss, Dr. Guido Serini, and Dr. Felix Randow, respectively. HA-ubiquitin construct was previously described (Polo et al., 2002). All other constructs described were engineered by site-directed mutagenesis or recombinant PCR and verified by sequencing.

HEK293T cells were cultured in Dulbecco's Modified Eagle's Medium (DMEM, Lonza) containing 10% fetal calf serum and 2 mM L-glutamine. Transient transfections were performed using Lipofectamine (Life Technologies) according to the manufacturers' instruction.

Protein Expression and Purification. *Escherichia coli* expression constructs for myosin VI (including MyUb (G1080-H1122 and G1080-R1131), linker- α 2-MyUb (R1050-R1131), MIU (Q998-S1025), iso3 (Q998-A1071), and iso3 (Q998-R1131) were fused to glutathione S-transferase (GST) and a PreScission protease cleavage site for ease of purification. Cells were grown at 37°C to OD₆₀₀ of 0.5-0.6 and protein expression induced by 0.4 mM IPTG at 17°C overnight. Samples were purified by affinity chromatography with glutathione sepharose resin followed by size exclusion chromatography. Monoubiquitin and its mutants (G76C, K11R, K48R, and K63R) were expressed, purified, and K11-, K48- and K63-linked chains conjugated as described previously (Bremm and Komander, 2012; Raasi and Pickart, 2005). Briefly, 0.1 μ M E1, 12 μ M UBE2S or 8 μ M Ubc13:Mms2 or 20 μ M E2-25K, 300 μ M G76C (proximal ubiquitin) and K11R or K63R or K48R (distal ubiquitin) was incubated together in 50 mM Tris-HCl (pH 7.6), 5 mM MgCl₂, 2.5 mM ATP (plus regenerating system), 0.6

U/mL inorganic pyrophosphatase, and 0.5 mM DTT. Reactions were incubated for 4 hours at 37°C and quenched with 5 mM of DTT and 1 mM EDTA. For purification, the pH was lowered to 4.5 by adding 1/5 volume of 2N acetic acid. Diubiquitin was eluted from a cationic exchange column by a linear gradient of NaCl (0-1M) in Buffer A (50mM ammonium acetate, pH 4.5, 1mM EDTA, 5mM DTT), with 20-40 column volumes. Peak fractions of diubiquitin were pooled together and dialyzed in storage buffer. All ¹⁵N- and ¹³C-labeled samples were produced in M9 media with ¹⁵N ammonium chloride and/or ¹³C glucose. Synthesis of asymmetrically labeled diubiquitin was carried out by using ¹³C- or ¹³C, ¹⁵N labeled monoubiquitin where desired.

GST Pull-down Experiments. 2 μM GST-fusion proteins were immobilized onto glutathione sepharose resin and incubated with 0.5 μg polyubiquitin chains, 1 mg HEK293T total cell lysate, or 200 μg of transfected HEK293T total cell lysate for 1 hour at 4°C in JS buffer (50 mM Hepes pH 7.5, 50 mM NaCl, 1.5mM MgCl₂, 5mM EGTA, 5% glycerol and 1% Triton X-100). After four washes with JS buffer, proteins were loaded in pre-cast 4-12% gradient gels (Biorad). Detection was performed by immunoblotting with specific antibodies. Ponceau-stained membranes were used to assess GST-fusion protein loading. For ubiquitin detection, Immobilon-P membranes (Millipore) membranes were treated with denaturing solution (6 M guanidine hydrochloride, 20 mM Tris-HCl pH 7.4, 1 mM PMSF, 5 μM β-mercaptoethanol) for 30 min at 4°C. After extensive washes with Tris-buffered saline (TBS), membranes were blocked in TBS buffer containing BSA (5%) for 6 hours and then incubated with anti-ubiquitin antibody (P4D1 or ZTA10) for 1 hour, followed by detection.

For the binding experiment shown in Figure 5C, lysate of HEK293T cells transfected with GFP-optineurin was immunoprecipitated with GFP-Trap (Chromotek). After four washes in JS buffer, GFP proteins were quantified by Coomassie. Beads corresponding to 1 μM of GFP proteins were used to pulldown 5 μM of GST, GST-MyUb WT or I1104A mutant eluted from the beads. Washes and detection were performed as described before.

NMR Spectroscopy. Standard NMR experiments and techniques were used to solve the structures of the myosin VI constructs and the MyUb complex with K63-linked diubiquitin, as we describe in the review articles (Chen and Walters, 2012; Walters et al., 2001). NMR experiments were acquired at 10°C (unless otherwise mentioned) on Bruker 600, 700, 800, 850, or 900 MHz spectrometers equipped with gradient cryoprobes. ¹⁵N-, or ¹³C, ¹⁵N-labeled samples used for titration experiments ranged from 0.1 to 0.2 mM, whereas experiments acquired for structure determination of MyUb (G1080-H1122 or G1080-R1131), iso3 (Q998-A1071), and MyUb:K63-linked diubiquitin were performed with 0.3 to 0.8 mM samples. All experiments were conducted in 20 mM sodium phosphate buffer (pH 6.5), 50 mM sodium chloride, 2 mM DTT, 0.01 % NaN₃, and 10 % ²H₂O / 90 % ¹H₂O (NMR buffer). 2D [¹H, ¹⁵N]-HSQC and 3D HNCO, HN(CA)CO, HNCA, HN(CO)CA, HNCACB, and CBCA(CO)NH spectra were collected for ¹⁵N, ¹³C MyUb (G1080-H1122 and G1080-R1131) and iso3 (Q998-A1071) and used for backbone ¹H, ¹⁵N, and ¹³C assignments. Side chain ¹H and ¹³C assignments were obtained by 2D [¹H, ¹³C]-HSQC and 3D HBHA(CO)NH, H(CCCO)NH, (H)CC(CO)NH, HCCH-COSY, HCCH-TOCSY, and (H)CCH-TOCSY spectra, also collected on all three myosin VI constructs with ¹⁵N and ¹³C labeled samples. Assignments were checked for consistency with 3D ¹⁵N/¹³C –NOESY-HSQC spectra recorded with mixing times of 120 ms; these NOESY spectra were acquired on ¹⁵N and ¹³C MyUb (G1080-H1122 and G1080-R1131), iso3 (Q998-A1071) and also on ¹⁵N and ¹³C MyUb (G1080-H1122) complexed with equimolar K63-linked diubiquitin. The assigned NOE interactions were used to derive distance constraints that were used in the structure calculations. Intermolecular distance restraints were recorded on ¹⁵N, ¹³C MyUb mixed with equimolar unlabeled K63-linked diubiquitin by using a 3D ¹³C/¹⁵N half-filtered NOESY experiment (120 ms). Selectivity for specific ubiquitin moieties was achieved by 3D ¹³C-half-filtered NOESY experiments (120 ms) acquired with either the proximal or distal ubiquitin ¹³C-labeled and MyUb unlabeled, as we describe previously (Chen and Walters, 2012).

Structure Determination. Table 1 displays structural statistics for MyUb (G1080-H1122), MyUb (G1080-R1131), MyUb (G1080-H1122):K63-linked diubiquitin, and iso3 Q998-A1071. NMR spectra were processed with NMRPipe and analyzed with KUIRA

(Kobayashi et al., 2007) and SPARKY. CYANA2.1 (Guntert, 2004) was used for automated NOE assignment and to calculate the structures by torsion angle dynamics; each NOE assignment was manually inspected and confirmed or corrected. Dihedral angle restraints were derived by TALOS (Cornilescu et al., 1999). The structure of MyUb:K63-linked diubiquitin was calculated with intramolecular restraints for ubiquitin (PDB: 1D3Z) that maintain its fold as well as our experimental restraints for free MyUb (G1080-H1122) and manually assigned intermolecular distance restraints. A total of 100 structures were independently calculated for MyUb (G1080-H1122), MyUb (G1080-R1131), iso3 Q998-A1071, and MyUb (G1080-H1122):K63-linked diubiquitin, and the twenty conformers with the lowest target-function values were selected for refinement with Xplor-NIH. Structures were evaluated with PROCHECK-NMR (Laskowski et al., 1996), visualized with MOLMOL (Koradi et al., 1996), and figures generated by PYMOL (The PyMOL Molecular Graphics System, <http://www.pymol.org/>).

SUPPLEMENTAL REFERENCES

Bremm, A., and Komander, D. (2012). Synthesis and analysis of K11-linked ubiquitin chains. *Methods in molecular biology* 832, 219-228.

Chen, X., and Walters, K.J. (2012). Identifying and studying ubiquitin receptors by NMR. *Methods in molecular biology* 832, 279-303.

Cornilescu, G., Delaglio, F., and Bax, A. (1999). Protein backbone angle restraints from searching a database for chemical shift and sequence homology. *Journal of biomolecular NMR* 13, 289-302.

Guntert, P. (2004). Automated NMR structure calculation with CYANA. *Methods Mol Biol* 278, 353-378.

Kobayashi, N., Iwahara, J., Koshiba, S., Tomizawa, T., Tochio, N., Guntert, P., Kigawa, T., and Yokoyama, S. (2007). KIJIRA, a package of integrated modules for systematic

and interactive analysis of NMR data directed to high-throughput NMR structure studies. *Journal of biomolecular NMR* 39, 31-52.

Koradi, R., Billeter, M., and Wuthrich, K. (1996). MOLMOL: a program for display and analysis of macromolecular structures. *Journal of molecular graphics* 14, 51-55, 29-32.

Laskowski, R.A., Rullmann, J.A., MacArthur, M.W., Kaptein, R., and Thornton, J.M. (1996). AQUA and PROCHECK-NMR: programs for checking the quality of protein structures solved by NMR. *Journal of biomolecular NMR* 8, 477-486.

Polo, S., Sigismund, S., Faretta, M., Guidi, M., Capua, M.R., Bossi, G., Chen, H., De Camilli, P., and Di Fiore, P.P. (2002). A single motif responsible for ubiquitin recognition and monoubiquitination in endocytic proteins. *Nature* 416, 451-455.

Raasi, S., and Pickart, C.M. (2005). Ubiquitin chain synthesis. *Methods in molecular biology* 301, 47-55.

Walters, K.J., Ferentz, A.E., Hare, B.J., Hidalgo, P., Jasanoff, A., Matsuo, H., and Wagner, G. (2001). Characterizing protein-protein complexes and oligomers by nuclear magnetic resonance spectroscopy. *Methods in enzymology* 339, 238-258.